Vanishing point attracts gaze in free-viewing and visual search tasks

Ali Borji[a,*], Mengyang Feng[b], Huchuan Lu[b]

[a] *Center for Research in Computer Vision, Department of Computer Science, University of Central Florida, Orlando, USA*
[b] *Department of Electrical Engineering, Dalian University of Technology, Dalian, China*

Abstract

Several structural scene cues such as gist, layout, horizontal line, openness and depth have been shown to guide scene perception (e.g., Oliva & Torralba (2001); Ross & Oliva (2009)). Here, to investigate whether the vanishing point (VP) plays a significant role in gaze guidance, we ran two experiments. In the first one, we recorded fixations of 10 observers (4 female; mean age 22; SD=0.84) freely viewing 532 images, out of which 319 had a VP (shuffled presentation; each image for 4 seconds). We found that the average number of fixations at a local region (80×80 pixels) centered at the VP is significantly higher than the average fixations at random locations (t-test; n=319; $p < 0.001$). To address the confounding factor of saliency, we learned a combined model of bottom-up saliency and VP. AUC score of our model (0.85; SD=0.01) is significantly higher than the original saliency model (e.g., 0.8 using AIM model by Bruce & Tsotsos (2005), t-test; p= 3.14e-16) and the VP-only model (0.64, t-test; $p < 0.001$). In the second experiment, we asked 14 subjects (4 female, mean age 23.07, SD=1.26) to search for a target character (T or L) placed randomly on a 3×3 imaginary grid overlaid on top of an image. Subjects reported their answers by pressing one of the two keys. Stimuli consisted of 270 color images (180 with a single VP, 90 without). The target happened with equal probability inside each cell (15 times L, 15 times T). We found that subjects were significantly faster (and more accurate) when target appeared inside the cell containing the VP compared to cells without the VP (median across 14 subjects 1.34 sec vs. 1.96; Wilcoxon rank-sum test; $p = 0.0014$). Response time for the VP cells were also significantly lower than response time on images without VP (median 2.37; $p < 0.001$). These findings support the hypothesis that vanishing point, similar to face, text (Cerf et al., 2009), and gaze direction (Borji et al., 2014) guides attention in free-viewing and visual search.

Keywords:
visual attention, eye movements, bottom-up saliency, free viewing, visual search, vanishing point, global context, gist

1. Introduction

Visual attention is crucial in understanding complex scenes and processing an enormous amount of information (around 10^8 bits) bombarding our retina each second. Primates use focal visual attention and rapid eye movements to analyze complex visual inputs in real-time, in a manner that highly depends on behavioral priorities and goals. Studies of physiology and psychophysics have proposed that several factors such as *bottom-up cues*, *nature of the target*, and *knowledge of task* play important roles in guiding attention and eye movements. We briefly explain these cues in the following.

Bottom-up cues guide attention based on low-level image-based features. Such cues make a red dot more salient among a set of blue dots. According to the Feature Integration Theory (FIT) by Treisman & Gelade (1980), several feature maps such as color, orientation, and intensity are computed in parallel across the visual field and are then combined to guide the attention. Koch and Ullman (Koch & Ullman, 1987)

*Corresponding author
Email addresses: aborji@crcv.ucf.edu (Ali Borji), archerfmy@163.com (Mengyang Feng), lhchuan@dlut.edu.cn (Huchuan Lu)

later introduced a computational architecture to generate a master saliency map and proposed a selection process to sequentially deploy attention to spatial locations in decreasing order of their salience. Several computational attention models have been proposed since then to detect bottom-up salient regions that stand out from their surroundings in an image (Itti et al., 1998; Bruce & Tsotsos, 2005; Borji & Itti, 2013; Borji et al., 2013b). These models have been shown to reliably predict fixations in free viewing of natural scenes (Parkhurst et al., 2002; Bruce & Tsotsos, 2005; Borji et al., 2013b, 2012).

Prior knowledge of the target facilitates target detection in visual search tasks (See Zelinsky (2008); Chen & Zelinsky (2006)). The guided search theory (Wolfe, 2007) proposes that attention can be biased towards targets of interest by modulating the relative gains through which different features contribute to attention. Psychophysics experiments have shown that knowledge of the target contributes to an amplification of its salience. For example, Blaser et al. (1999) reports that white vertical lines become more salient if we are looking for them. Some studies have shown that better knowledge of the target leads to faster search, e.g., seeing an exact picture of the target is better than seeing a picture of the same semantic type or category as the target (Kenner & Wolfe, 2003; Maxfield et al., 2014). Physiology experiments have shown that target search modulates neural activity by enhancing the responses of neurons tuned to the location and features of a stimulus (Treue & Trujillo, 1999; Saenz et al., 2002; Martinez-Trujillo & Treue, 2004; Bichot et al., 2005). Navalpakkam and Itti have investigated computational and behavioral underpinnings of these processes (Navalpakkam & Itti, 2007, 2005, 2006) and have proposed models to bias the low-level visual system with the known features of the target to make the target more salient (a.k.a the optimal gain theory). Borji & Itti (2014b) have studied how parameters of neurons in a neural population should be optimally biased to search for a target.

Further, it has been shown that attention in the real world is mainly task-driven (Ballard et al., 1995; Hayhoe & Ballard, 2005; Borji & Itti, 2014a). The classic eye movement experiments of Yarbus et al. (1967) show drastically different patterns of eye movements over the same scene, depending on the task. He demonstrated a striking example of how a verbally-communicated task specification may dramatically affect attentional deployment and eye movements. He argued that variable spatio-temporal characteristics of scanpath for different task specifications exemplify the extent to which behavioral goals may affect eye movements and scene analysis. Another example in this regard is the study by Tanenhaus et al. (1995) who investigated the interplay between task demands (spoken sentence comprehension) and gaze control by tracking eye movements of subjects when they received ambiguous verbal instructions regarding manipulating objects on a table. Tanenhaus et al. demonstrated that visual context influenced spoken word recognition and syntactic processing when subjects had to resolve ambiguous verbal instructions by analyzing the visual scene and objects. These two studies indicate that visual attention and scene understanding are intimately interrelated and that gaze is controlled by task demands. In another work, Triesch et al. (2003) suggested that our brain may adopt a need-based approach, where only desired objects are quickly detected in the scene, identified and represented. In natural vision, bottom-up saliency, search template (object features), scene context and layout, and task demands interact with each other in guiding visual attention.

The geometry of a scene provides global contextual information that assists rapid scene analysis in visual search and navigation (Ross & Oliva, 2009). Structural cues such as layout, depth, openness, and perspective can be perceived in a short presentation of an image (Greene & Oliva, 2009; Schyns & Oliva, 1994; Joubert et al., 2007; Sanocki & Sulman, 2009). Further, global scene context or Gist[1] (Torralba et al., 2006) and layout[2] (Rensink, 2000) also guide attention to likely target locations in a top-down manner. Given a task such as "find humans in the scene", in addition to visual features representing the appearance of a person, the gist of the scene also guides the search process. For example, humans are more likely to be found on the sand, rather than on the sky, in a beach scene. Ehinger et al. (2009) proposed a model to linearly integrate three components (bottom-up saliency, gist, and object features) for explaining eye movements in

[1] An abstract spatial representation which is rich enough to recognize the semantic category of a scene, such as indoor office, outdoor beach, street, etc.

[2] A scene can be partitioned into coherent spatial regions based on semantic or visual similarity. For example, a typical beach scene can be represented by three regions: sky on top, water in the middle, and sand at the bottom.

looking for people in a database of about 900 natural scenes. Structural scene information has also been extensively modeled and utilized in several computer vision applications (e.g., geometry context (Hoiem et al., 2005) and Manhattan world (Coughlan & Yuille, 2003)). While influences of structural information on visual recognition (e.g., rapid scene categorization and understanding) have been studied, its role in visual attention has not yet been systematically explored.

Previous research has shown that drivers rely on the road tangent point (the point of the inner lane marking bearing the highest curvature in the 2D retinal image) when negotiating a bend. The bend radius (and hence the steering angle) relates in a simple geometrical fashion to the visible angle between the instantaneous heading direction of the car and the tangent point (Land & Lee, 1994). Drivers can easily use this strategy by looking at the tangent point and inferring the required steering angle from the rotation angle of their gaze and head. Driving by the tangent point has been observed from both normal and racing drivers in real world scenarios (Land & Lee, 1994; Land & Tatler, 2001; Chattington et al., 2007), as well as in simulated conditions (Wilson et al., 2008).

In summary, several cognitive cues that attract attention and guide eye movements in natural vision have been already discovered (e.g., color, texture, motion, face and text (Cerf et al., 2009), object center-bias (Nuthmann & Henderson, 2010), scene center-bias (Tatler et al., 2005), cultural cues (Chua et al., 2005; Rayner et al., 2009), semantic distance (Hwang et al., 2011), and gaze direction (Castelhano et al., 2007; Borji et al., 2014)). Further, structural scene information such as global context, horizontal line[3], and openness (Torralba et al., 2006), scene layout (Rensink, 2000), and depth (Ouerhani & Hügli, 2000; Le Meur, 2011) have been shown to influence eye movements as well as human scene categorization (Friedman, 1979; Potter, 1976; Oliva & Torralba, 2001). Here, we systematically investigate the role of a particular type of scene structural information known as vanishing point (VP) and perspective on eye movements during free-viewing and visual search in natural scenes. In a graphical perspective, a *vanishing point* is a 2D point (in the image plane) which is the intersection of parallel lines in the 3D world (but not parallel to the image plane). In other words, the vanishing point is the spot to which the receding parallel lines diminish. In principle, there can be more than one vanishing point in the image. VP can commonly be seen in fields, railroads, streets, tunnels, forest, buildings, objects such as ladder (from looking bottom-up), etc. It has been used in camera calibration, 3D reconstruction as well as in painting.

[3]The line that separates the earth from the sky (a.k.a skyline). Observers are more likely to attend to visual items along the horizontal line (Le Meur, 2011).

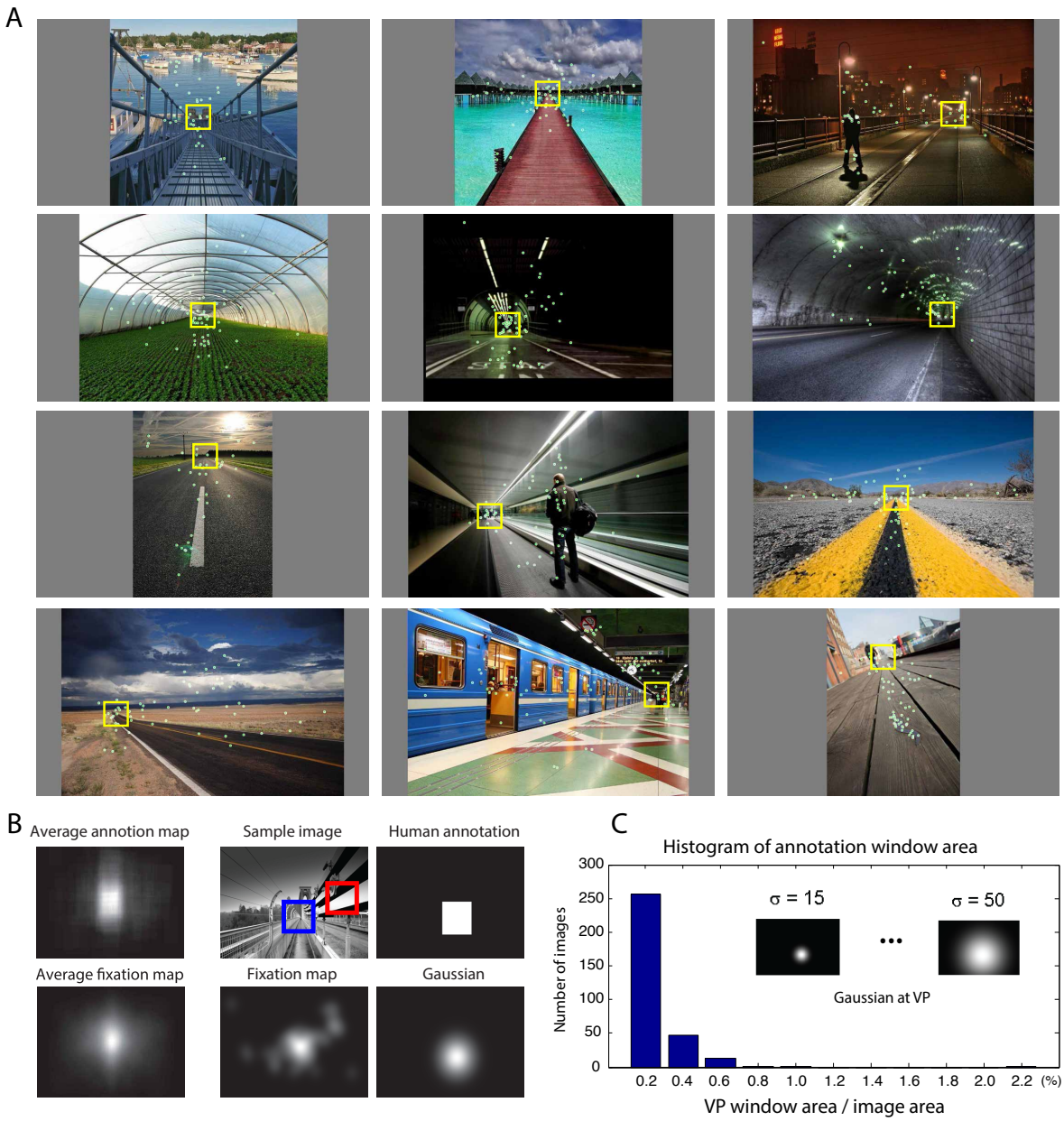

Figure 1: A) Example stimuli with vanishing points (yellow boxes) and fixations (dots) used in experiment one. These images were shown to observers shuffled among some other images without vanishing point to avoid viewing bias (i.e., strategy in viewing). For images with some highly salient items, vanishing point attracts less attention (e.g., 2nd image in the 4th row). B) Average VP annotation map and average fixation map over 319 images with VPs. A sample image and its corresponding human VP annotation, eye movements of 10 observers, and Gaussian blob centered at the VP is also shown. The inset shows two squares with size 80×80 pixels (blue=square centered at the VP location, red=square centered at the VP location of another randomly chosen image). C) Histogram of VP window size. About 82% of VP bounding boxes have a size smaller than 0.2% of the image area. Inset shows two Gaussian blobs with smallest and largest σ values.

2. Experiment one: free viewing

2.1. Methods

2.1.1. Stimuli

We collected 319 images with vanishing points from the Web, MIT300 (Judd et al., 2012) and DUT-OMRON (Yang et al., 2013) datasets from different categories (indoor, outdoor, man-made, natural, street, etc). These images have only one vanishing point. We asked two subjects to annotate the VP location[4]. They were shown images with the maximum resolution[5] of 400×300 pixels, and were asked to mark the VP with a bounding box of an arbitrary size. The average height and width of the VP bounding boxes were 10 and 14 pixels, respectively. In the latter analyses, we only use the center of the bounding boxes.

Since showing only images with a VP may guide observers to adopt a viewing strategy, we collected additional 213 images without vanishing points and shuffled them among images with VPs. Therefore, viewers would not know in advance whether a presented image would contain a VP. In total, we had 532 images to record human fixations (319 with VP and 213 without). In what follows, only images containing vanishing points are analyzed. For presenting to subjects, images were resized to 1920×1080 pixels by adding gray margins to them while preserving the aspect ratio.

Figure 1.A shows examples of our stimuli, annotated vanishing points, as well as fixation locations. Figure 1.B shows the average annotation map as well as the average fixation map over 319 images with VPs. Both of these maps have maximum activation near the image center making center-bias a potential confounding factor for our hypothesis. We will address this confound extensively in our analyses. Figure 1.C shows the histogram of VP window size (bounding box). About 82% of annotated VP bounding boxes have a size smaller than 0.2% the image area.

2.1.2. Observers

Observers were undergraduates from different majors (6 male, 4 female). Mean observer age was 22 (min=21, max=24, median=22, SD=0.84). Observers had normal or corrected-to-normal vision and received course credits for participation. They were naive to the purpose of the experiment and had not previously seen the stimuli.

2.1.3. Procedure

Following the fixation cross, an image was shown for 4 seconds followed by a gray screen for 3 seconds. Observers sat 60 cm away from a $19''$ LCD monitor such that scenes subtended approximately $37.6^\circ \times 24^\circ$ of the visual field. A chin rest was used to stabilize head movements. Stimuli were presented at 60Hz at a resolution of 1920×1080 pixels (with added gray margins while preserving the aspect ratio). Eye movements were recorded via a Tobii X1 Light Eye Tracker at a sample rate of 30Hz. The eye tracker was calibrated using 5 points calibration at the beginning of each recording session. Images were presented to observers in a random order. Observers were instructed to simply watch and enjoy the pictures (free viewing task).

3. Model-free analysis

In our first analysis in this section, we compute and compare the density of fixations inside the VP and random bounding boxes of the same size (80×80 pixels). We take the center of the annotated rectangles and draw an 80×80 square at that location[6]. To generate a random bounding box for an image, we use the VP bounding box of another randomly chosen image. This way, random locations have the same central bias as the VPs.

[4]Subjects were highly consistent in their selection of vanishing point locations ($R^2 = 0.99$). Please see appendix A.

[5]The largest dimension was resized to 400 pixels. The smaller dimension was resized such as to preserve the aspect ratio and thus may sometimes exceed 300 pixels.

[6]Our investigation with other bounding box sizes results in the same conclusions.

An average number of fixations inside the VP squares is 33.1 (SD=15.5) which is significantly higher than the average number of fixations at random locations (19.8; SD=16.2) using t-test (n=319; p = 2.98 e-35). This implies that fixations are driven to vanishing points (See Figures 2.A and 2.B).

In our second analysis, we repeat the first analysis with saliency maps (Figure 2). We find that average saliency (using Itti (Itti et al., 1998), AIM (Bruce & Tsotsos, 2005) and BMS (Zhang & Sclaroff, 2013) models) in the VP square is significantly higher than random squares (t-test; n=319; p=4.23e-13 using the Itti model, p=2.03e-08 using the AIM model and p=0.02 using the BMS model). Please see Figures 2.C and 2.D.

One may argue that the higher number of fixations and map activations using the human fixation map at vanishing points compared to random points, could be because of higher saliency around vanishing points (as shown above). In other words, feature congestion at VP induces higher low-level image-based saliency and drives attention. This makes bottom-up saliency a potential confounding factor for our hypothesis here. To address this confound, we measured the ratio of average activation at VP versus random locations using saliency models as well as the blurred human fixation map (by convolving with a small Gaussian blob of $\sigma = 10$ pixels; Figure 1.B). The ratio using the human fixation map is 1.5 which is higher than ratios using models (1.3 for Itti, 1.2 for AIM, 1.1 for BMS). This means that while saliency plays a role, it can not fully account for the VP effect. We will investigate this further in the next section by utilizing a model-based analysis.

4. Model-based analysis

In the previous analyses, we showed that saliency at the VP is higher than random locations. To investigate whether attraction of fixations towards vanishing point is solely due to the higher saliency at VP or there is a significant additional value, we perform a model-based analysis. If the vanishing point offers redundant information to what saliency already offers, then explicit emphasis on the vanishing point should not add significant prediction power. Similar analyses have been pursued in the past to study whether other types of cues such as face and text (Cerf et al., 2009), object center-bias (Borji & Tanner, 2015), and gaze direction (Borji et al., 2014; Parks et al., 2015) guide eye movements and attention.

4.1. Learning a combined model of saliency and vanishing point

To learn a combined model of saliency and vanishing point, we represent each image pixel as a vector X = [s v] where s is the output of a bottom-up saliency model[7] and v is the value from the vanishing point map (VP). VP map is modeled as a variable size Gaussian placed at the vanishing point as shown in Figure 1[8]:

$$VP(x,y) = \frac{1}{2\pi\sigma_{vp}^2} e^{-\frac{(x-i)^2+(y-j)^2}{4\sigma_{vp}^2}} \tag{1}$$

where (i, j) is the coordinate of the annotated vanishing point and σ_{vp} is the (variable) standard deviation of the Gaussian blob.

We aim to learn function $\phi(\mathrm{X}) = W^T\mathrm{X} + b$ which is a binary classifier determining whether a particular image pixel with feature vector X should be attended or not (i.e., $\phi(\mathrm{X}) \in \{-1, 1\}$). To do so, we utilize an ordinary support vector machine (SVM; Cortes & Vapnik (1995)) with a linear kernel. For a test pixel, we assign the real value $m = W^T\mathrm{X} + b$ as the label of the pixel[9]. Final saliency values are then normalized for each map (i.e., (m - min) / (max - min)). We deliberately avoid using complicated non-linear learning functions, since we are interested in the exclusive added value of the vanishing point.

We choose 50 random images to train the SVM and use the remaining 269 images for testing. This procedure is repeated 20 times and then the average is computed (i.e., cross-validation). We randomly select

[7]We chose Itti, AIM and BMS models since they use purely bottom-up cues such as orientation or color and exclude high-level features such as face or text.

[8]We experimentally verified that the Gaussian form of VP works better than square or circle.

[9]This model is essentially similar to learning a linear model: $\alpha S + (1 - \alpha)VP$.

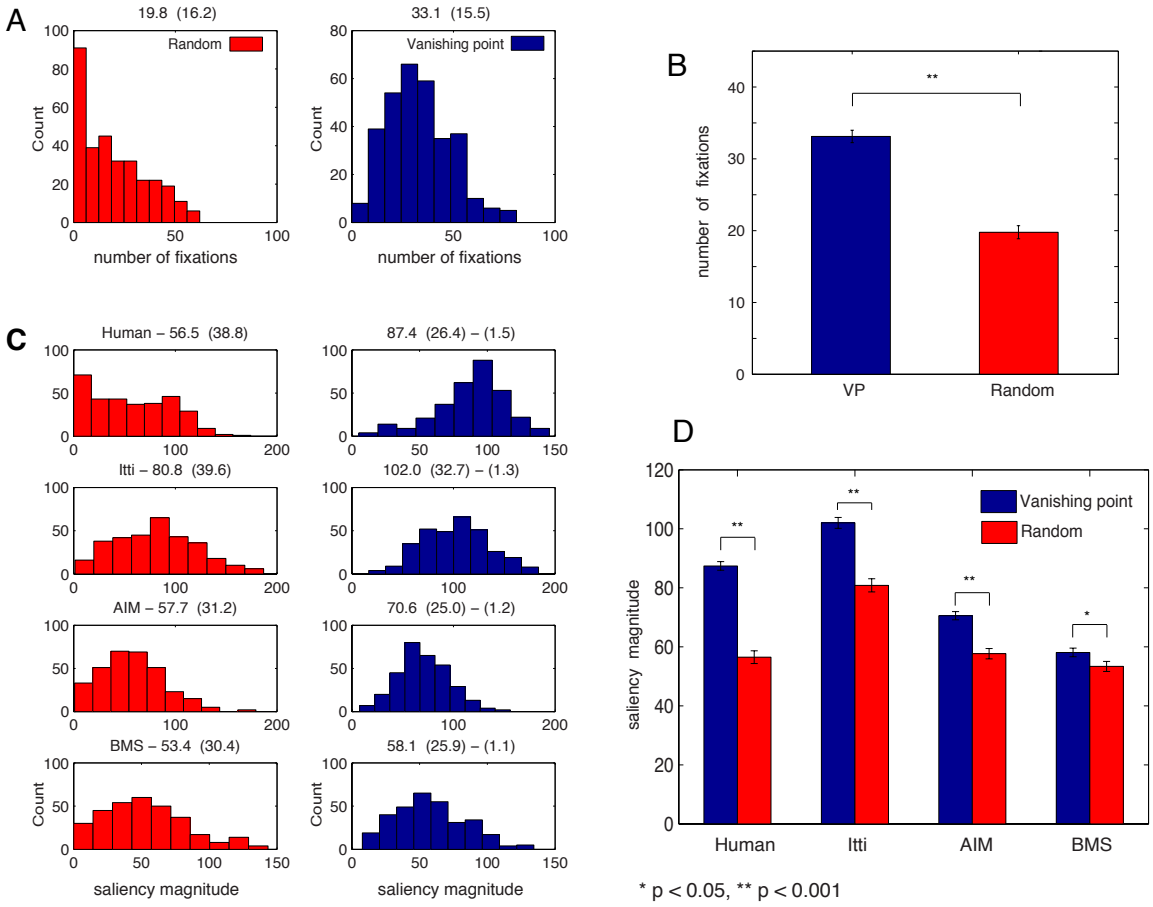

Figure 2: Results of the first experiment. A) Histogram of fixations at random (left column) and annotated VP squares (80 × 80 pixels). Plot titles show mean and standard deviations (in parentheses). B) The mean number of fixations at VP and random squares (sampled with the same bias as VP annotations to account for center-bias). The difference is statistically significant using t-test (n=319). C) Histogram of saliency map activations at VP and random squares (see Figure 1.B) using human saliency map (fixation map convolved with a small Gaussian blob with $\sigma = 10$ pixels). The second parenthesis on the title of the right bar column shows the ratio of the means (i.e., mean-at-VP/mean-at-random). D) Differences in VP and random squares means. All differences are statistically significant using t-test. Error bars show standard error of the mean (s.e.m).

50 pixels respectively from fixated locations and non-fixated locations, yielding 100 samples (50 positive samples and 50 negative samples) for each training image, i.e., 5000 training samples in total. We learn the combined models (e.g., AIM + VP, BMS + VP, and Itti + VP) and compare them with the original bottom-up saliency models. For a fair comparison, we optimize models by sweeping[10] σ_{vp} from 15 to 50 pixels and find the σ where performance peaks[11]. Please see Figure 3.A.

4.2. Model evaluation

Table 1 summarizes the test results using three types of scores: Area under the curve (AUC), Normalized scanpath saliency(NSS) proposed by Peters et al. (2005) and linear correlation coefficient (CC). Please see Borji & Itti (2013) for a detailed definition of these scores in the context of fixation prediction. We make three observations explained below (See Figure 3.A).

First, we observe that the VP performs significantly above chance in predicting fixations using all three scores (Table 1, last column). Using the AUC score, VP map offers at least 43% improvement versus chance.

Second, adding VP to models significantly outperforms baseline models using three scores (M +VP vs. M; Table 1, fifth column). We observe more than 8.5% improvement in performance using the AUC score (more than 48% using NSS and more than 52.5% using CC). This result confirms our hypothesis that VP offers significant additional prediction power than bottom-up saliency.

Third, M + VP model outperforms the VP model using the AUC score but performs slightly lower than VP using NSS and CC scores due to a different amount of activation generated by these models (Table 1, fourth column). This comparison is not very relevant to our hypothesis here as it compares VP and bottom-up saliency. Marginal improvement of M + VP over VP (and sometimes lower performance), hints towards the strong attraction of gaze towards the vanishing point such that emphasizing more on bottom-up salient items degrades the accuracy. Nonetheless, results from fourth and fifth columns of Table 1 confirm that both bottom-up saliency and vanishing point contribute statistically significantly in guiding attention and gaze in free viewing and none in a subset of the other one.

4.3. Addressing center-bias

It has been shown that human observers tend to preferentially look near the center of the image due to reasons such as viewing strategy or photographer bias (the tendency of photographers to frame interesting objects at the center of the picture). This phenomenon is known as center bias and has challenged researchers in testing hypotheses in eye movement studies and comparing saliency models (Tatler et al., 2005; Tseng et al., 2009; Borji et al., 2013a). In this section, we address this confounding factor in detail. Notice that VP happens at the center of some of our images.

We perform two comparisons. First, we investigate whether VP and CG (Central Gaussian) models offer non-redundant information. CG is a model that is a Gaussian blob located at the center of the image. Notice that both models have been optimized by first optimizing for σ of the VP and then optimizing for σ of the CG model. The scatter plot in Figure 3.B shows that for 97 of 269 test images, the VP model wins over the CG model. Inspecting images in which VP wins, we see that VP falls off the image center and observers look at the VP location. For images where CG wins, there is either: i) a salient object at the image center, ii) a VP at the image center, or iii) scene contains mainly background clutter. In the latter case, observers tend to look at the center as there is not much interesting peripheral stuff to look at.

Second, we compare the M + CG + VP model versus the M + CG model. The rationale behind this comparison is to see whether VP boosts the performance of the augmented (with CG) model. Figure 3.C shows performance increase for 221 images (about 82% of images). The third column in Table 1 shows the quantitative results and statistical tests (t-test; n=269). The difference between M + CG + VP and M + CG models is statistically significant using all bottom-up saliency models and scores. These two comparisons confirm that vanishing point and central bias are two different non-overlapping cues that attract fixations and guide attention.

[10]Previous research has shown than smoothing impacts saliency model performance (Borji et al., 2013a; Borji & Itti, 2012).
[11]Please note that for different models, different VP σ leads to the best M + VP performance.

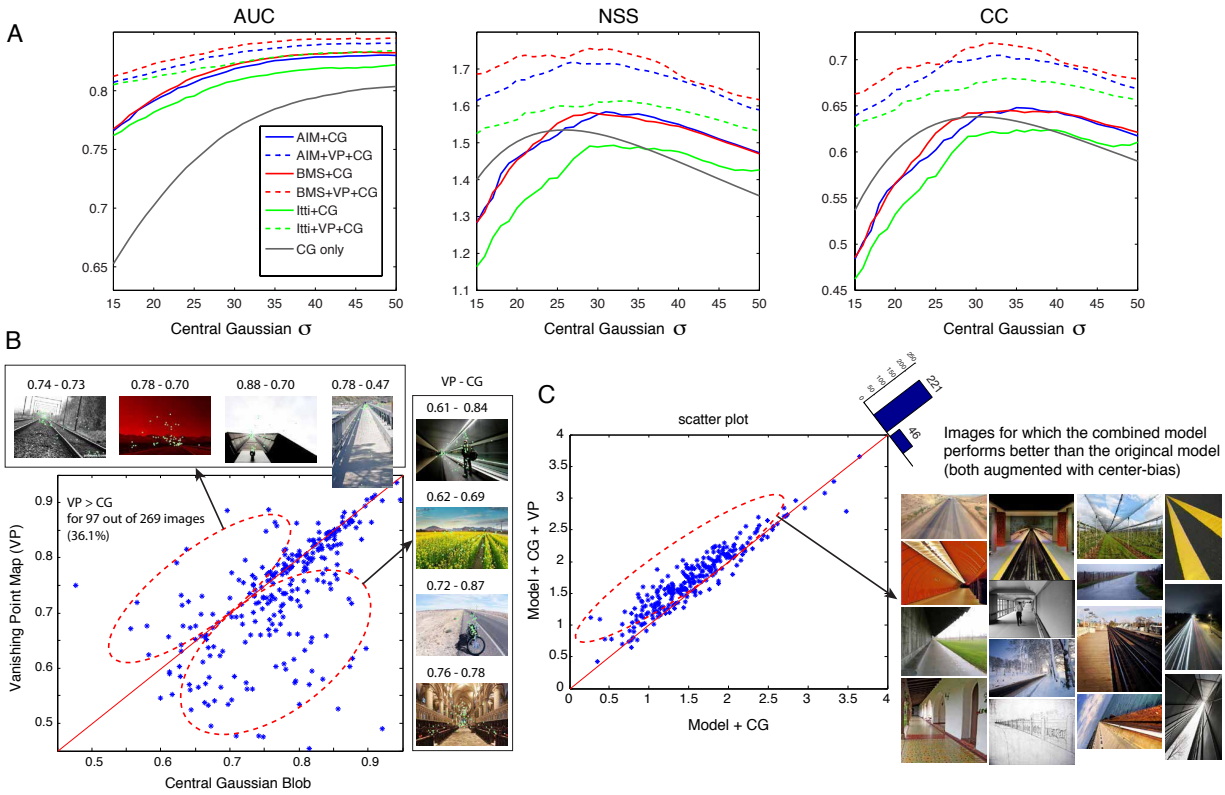

Figure 3: A) The performance of models using AUC, NSS and CC scores with varying Gaussian σ. The x axis indicates the σ of the central Gaussian blob. The σ of the VP Gaussian blob is fixed to the best sigma for each model. B) AUC score of the VP map versus the CG central Gaussian (CG) map using the best σ (here both σ values are 31 pixels). Each dot represents one image. Some examples above and below diagonal are shown. C) Scatter plot of Model + CG versus Model + CG + VP using the NSS score. This plot shows the added value of VP over the original model taking into account the center bias confound. This plot also indicates that the added value is not due to the center-bias. For 221 images, we observe performance improvement. Vanishing point usually happens off the center on these images. We did the same analysis by plotting the Model + VP versus M and observed performance improvement for 243 of the images (not shown).

Score	Model = M	M + CG + VP vs. M + CG	M + VP vs. VP	M + VP vs. M	VP vs. Chance
AUC	AIM	0.833 vs 0.819 (1.7%)	0.793 vs 0.739 (7.3%)	0.793 vs 0.720 (10.13%)	0.739 vs 0.5 (47.8%)
	BMS	0.837 vs 0.823 (1.7%)	0.798 vs 0.719 (11%)	0.798 vs 0.711 (12.2%)	0.719 vs 0.5 (43.8%)
	Itti	0.826 vs 0.811 (1.84%)	0.792 vs 0.756 (4.7%)	0.792 vs 0.730 (8.5%)	0.756 vs 0.5 (51.2%)
NSS	AIM	1.695 vs 1.545 (9.7%)	1.467 vs 1.450 (1.2%)	1.467 vs 0.953 (53.9%)	1.450 vs 0
	BMS	1.751 vs 1.587 (10.33%)	1.543 vs 1.508 (2.3%)	1.543 vs 0.916 (68.4%)	1.508 vs 0
	Itti	1.592 vs 1.445 (10.2%)	1.361 vs 1.381 (-1.4%)	1.361 vs 0.918 (48.25%)	1.381 vs 0
CC	AIM	0.697 vs 0.628 (11%)	0.584 vs 0.598 (-2.3%)	0.584 vs 0.358 (63.12%)	0.598 vs 0
	BMS	0.720 vs 0.652 (10.42%)	0.609 vs 0.608 (0.16%)	0.609 vs 0.341 (78.5%)	0.608 vs 0
	Itti	0.672 vs 0.603 (11.44%)	0.563 vs 0.580 (-2.9%)	0.563 vs 0.369 (52.6%)	0.580 vs 0

Table 1: Scores of our combined model (Model + VP) vs. the original model and the VP-only channel. Numbers in parentheses are the performance improvement in percentages. Scores of the center-bias augmented models are also shown (third column). Differences are all statistically significant (t-test; n=269; $p < 0.05$) except the CC score of M + VP vs. VP using the Itti model ($p = .83$).

4.4. Qualitative evaluation

Here, we evaluate model prediction maps qualitatively. Figure 4 shows examples where our combined model performs poorly (i.e., M + VP scores lower than M). In almost all of these cases, an object off the vanishing point overrides the VP effect. For example, in the second row of the first column, a standing person in the metro station attracts gaze more than VP (the same is true for images in 1st row, 2nd column and 1st row, 3rd column).

Figure 5 shows examples where our combined model performs well. Scores of models are also shown. The original baseline models (AIM, BMS and Itti) fail to render the vanishing point salient in almost all of the shown cases. Augmented with VP, however, we see an improvement in the prediction power (Compare M + VP versus M). M + CG model also outperforms the M model. The best performance is achieved using the M + VP + CG model. This model however sometimes loses to the M + VP model as adding CG causes false positives in some cases. Comparing the VP and CG models (the last two columns) indicates that VP sometimes wins over CG, especially in cases where VP is off the image center.

4.5. Complementary analysis

In a complementary analysis, to investigate whether vanishing point guides attention in other tasks, we evaluate the performance of our combined model over existing datasets in the literature. Fourteen images with vanishing points were selected from the FIGRIM (Bylinskii et al., 2015) dataset and VP locations were annotated. FIGRIM images have been used for memorability testing to probe whether eye movements relate to whether a subject will later remember an observed image. Note that these images have been shown to observers among many other images without VP. Therefore, there is no bias towards looking at the vanishing point on these datasets. The performance of our combined model over these images is shown in Table 2. As it can be seen, our model performs better than original models using all three scores. Figure 6 shows an illustration over the FIGRIM dataset.

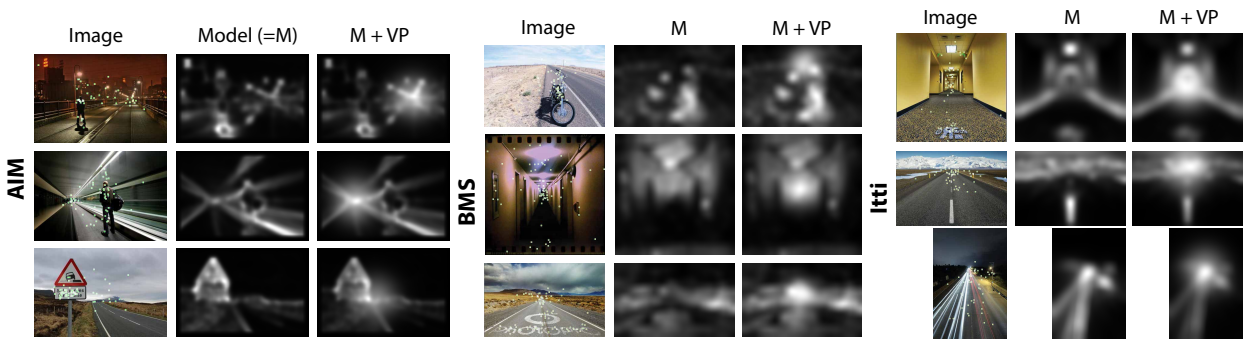

Figure 4: Qualitative evaluation: cases where our combined model performs poorly. In almost all of these cases, an object off the vanishing point overrides the VP effect and attracts fixations.

Score \ Model	AIM + VP	BMS + VP	ITTI + VP	SALICON + VP
AUC	0.837 (0.758)	0.854 (0.764)	0.846 (0.799)	0.825 (0.795)
NSS	1.731 (1.081)	1.851 (1.151)	1.716 (1.221)	2.611 (2.379)
CC	0.511 (0.308)	0.533 (0.321)	0.523 (0.363)	0.683 (0.614)
Best VP σ	31	27	37	16
W	[9.453, 6.693]	[10.716, 6.982]	[6.883, 6.931]	[16.222, 6.164]

Table 2: Maximum scores of our combined models over 14 images with vanishing points selected from the FIGRIM (Bylinskii et al., 2015) dataset. Numbers in parentheses are scores of the original models.

5. Experiment two: visual search

Our aim in this experiment is to investigate whether our findings from the free-viewing task generalize to other tasks. In particular, we attempt to see whether presence of a vanishing point attracts attention during visual search.

5.1. Methods

5.1.1. Stimuli

Our stimuli contain 270 color images, selected from images used in experiment one, 180 of which with vanishing points and 90 without. A target character (T or L) was placed randomly on a 3×3 imaginary grid overlaid on an image (See Figure 7.B, 4th row, 1st column). The target character occupies 0.80×0.67 degrees of the visual field. The target happened with equal probability (1/9) inside each cell (30 times: 15 times L, 15 times T). Twenty times, out of this 30, happened on images with a vanishing point (10 L, 10 T) and 10 times over images without a VP (5 L, 5T). Figure 7 shows example stimuli used in the visual search experiment.

5.1.2. Subjects

Fourteen subjects (10 male, 4 female) voluntarily participated in this experiment. Mean subject age was 23 (min=22, max=27, median=23, SD =1.27). All subjects were undergraduates from different majors. They were naive to the purpose of the experiment and had not previously seen the stimuli.

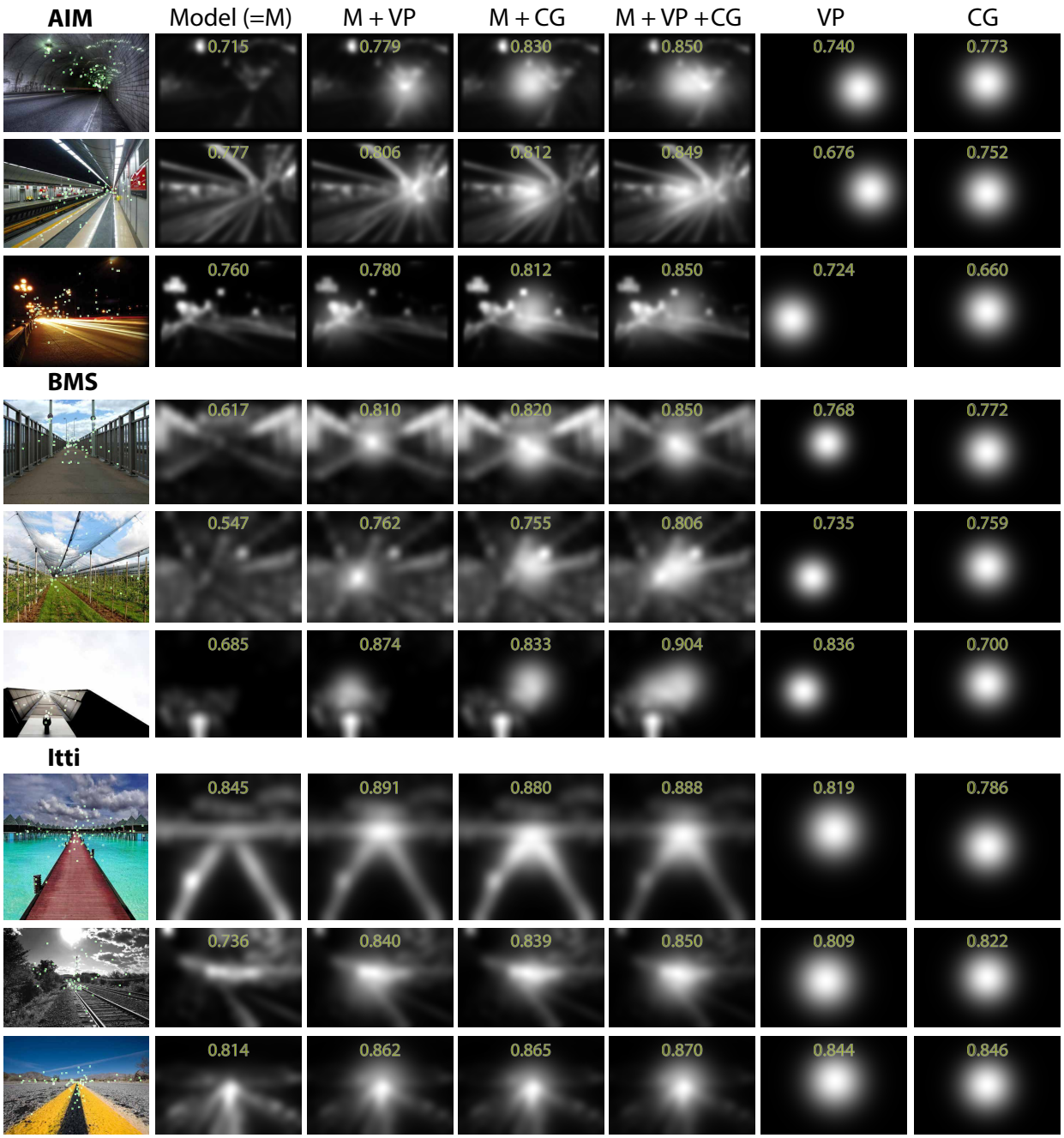

Figure 5: Qualitative evaluation: cases where our combined model performs well (using the AUC score).

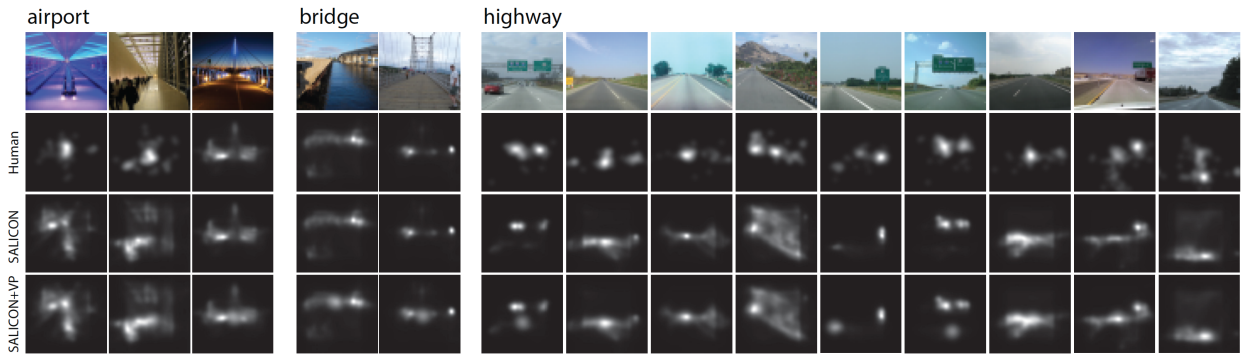

Figure 6: Illustration of predictions of the SALICON model (as one of the best existing saliency models (Bylinskii et al., 2014)) versus SALICON + VP model over images taken from the FIGRIM dataset.

5.1.3. Procedure

As in experiment one, observers sat 60 cm away from a 19″ LCD screen. Stimuli were presented at 60 Hz at a resolution of 1920 × 1080 pixels with added gray margins (dva 37.6° x 24°). Subjects were asked to search for the target character. They were instructed to report their answers by pressing one of two arrow keys (left arrow for T, right arrow for L). If no key was pressed after 10 seconds, trial automatically moved to the next one. Subjects were not asked to look at the center of the screen before each trial. The reason was to avoid preference towards the center where vanishing point usually happens[12]. Each stimulus was succeeded by a gray screen for 4 seconds. Overall, it took about 30 minutes for a subject to complete this task. We measured subjects' response times and accuracies.

5.1.4. Analysis and results

Figure 8 shows the results of the second experiment. Analyzing images with a VP, we found that all subjects[13] were significantly faster when target happened inside the cell containing the VP compared to cells without a VP (median across 14 subjects; 1.34 seconds vs. 1.96 seconds; Wilcoxon rank-sum test; p = 0.0014; Figure 8.A). Response time for the VP cells was also significantly lower than response time on images without VP (median 2.37; p= 4.77e-05). Response time on off-VP cells (over images with VP) was lower than response time on images without a VP (p=0.0072). This was unexpected since we anticipated that the VP would act as a distractor hence raising response time over off-VP grid cells. We attribute this to lower complexity of scenes with a VP as those scenes usually had relatively less clutter compared to images without a VP. Further, our images without a VP often contain faces, text and other salient stimuli that could act as distractors and attract fixations which in effect could raise the response time (See for example Figure 7.C). Notice, however, the important straight comparison related to our hypothesis is the response time and accuracy in VP vs. off-VP cells.

Median (and also mean) accuracies over subjects were above 95% (Figure 8.B). Accuracies for the target in VP cells were significantly higher than off-VP cells (medians 100% versus 97%; p=0.02) and images without a VP (median 95%; p=0.01). This result supports our hypothesis that vanishing point guides attention during visual search.

[12] To further alleviate center-bias, we cropped the images in such a way to distribute the vanishing point over the entire 3 × 3 grid on the image.

[13] See appendix B for results over individual subjects.

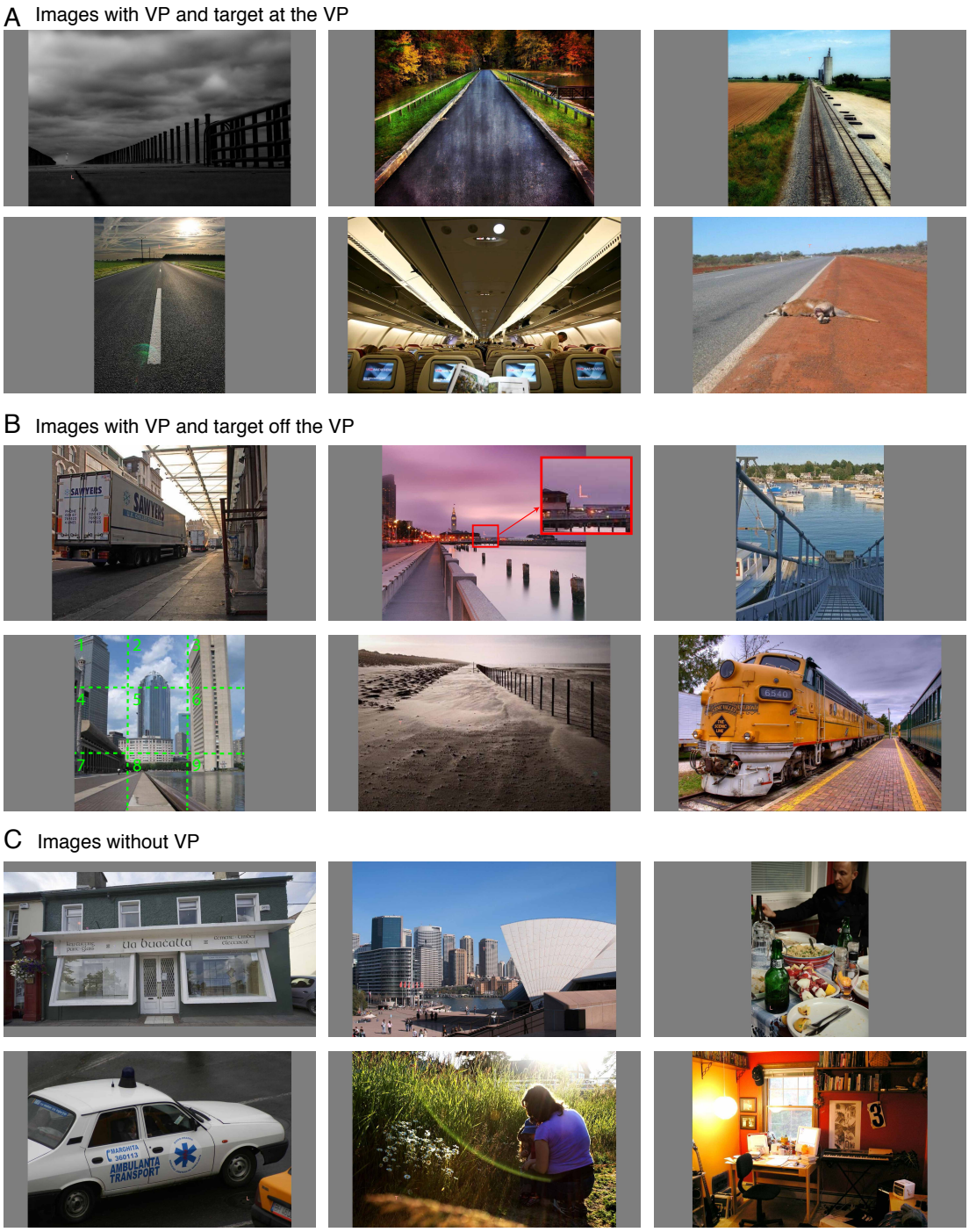

Figure 7: Stimuli used in the visual search experiment (270 images in total). A) Images with the target at the vanishing point, B) Images with vanishing point but target off the VP. The image in the 4th row, 1st column shows a 3×3 imaginary grid with the target at the center cell, C) Images without VP. The inset in the image in the 3rd row, 2nd column shows the zoomed out target region for better illustration. Try to see if you can locate the grid cell containing the target character (T or L) in images. (Answer key: A) 7, 2, 2, 2, 8, 2, B) 9, 5, 2, 6, 4, 9, C) 4, 5, 7, 9, 7, 7).

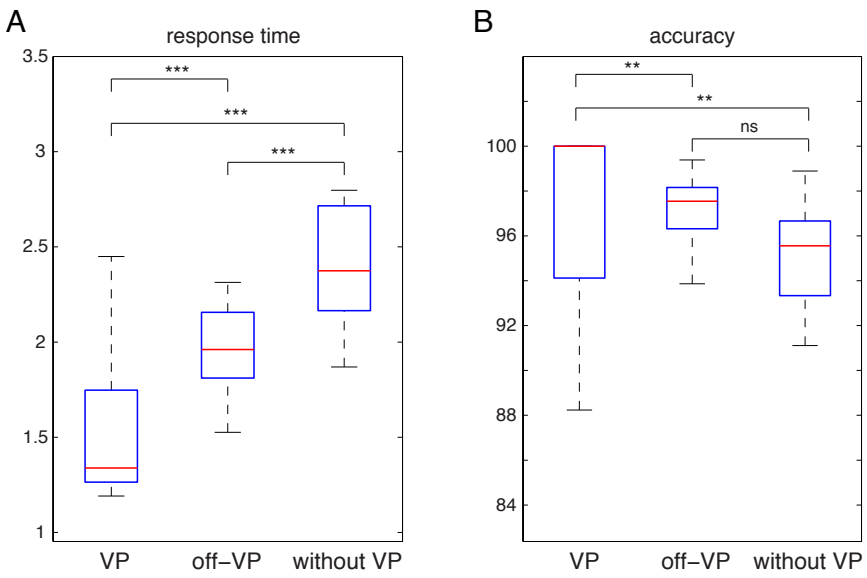

Figure 8: Results of the visual search experiment. A) Response time, b) Accuracy. *** = $p < 0.001$, ** = $p < 0.01$, ns = non significant (here p=0.055; almost significant).

6. Discussion

Our data shows that there is a guidance towards the vanishing point on images with a strong vanishing point. There might be a continuum between these types of examples, and those where the geometry defines a vanishing point that is out of frame, or wherein the images are less "tunnel" like. It would also be interesting to measure the vanishing point guidance on images with multiple vanishing points.

Is it a preference to fixate points having a greater perceived distance, or does the VP fixation preference reflect the contribution of a lower-level visual factor? By definition, the vanishing point is the point in infinity in the scene (3D world). So, it is very difficult to rule out the depth cue. However, there are often several points with depth at infinity which capture less attention compared to the vanishing point. A likely explanation for vanishing point preference could be a especial form of low-level processing similar to faces. Based on our findings, we suggest that there might be some fast dedicated neural mechanisms for computing vanishing point and perspective in the brain (for example neurons in cortical areas V4 or IT), similar to how faces and text are computed to guide attention. Indeed, it is known that there are face-selective neurons in the fusiform gyrus that contribute to guiding attention (McCarthy et al., 1997).

A finer grained analysis of fixations towards vanishing points might reveal interesting patterns. We notice that in some images (e.g., roads), there is a higher density of fixations and feature congestion beneath the vanishing point. Emphasizing more on these regions may further improve the prediction power of our combined model. Further, in some cases, fixations seem to be marked by a trail that leads towards the vanishing point which raises the question of whether an anisotropic profile for this bias factor might produce even stronger results.

As we showed in Section 4, the explicit addition of a vanishing point channel to a saliency model significantly improves the performance on images with vanishing points. Even the best existing saliency model (SALICON by Jiang et al. (2015)), trained on a large amount of data falls short in explaining fixations driven by the vanishing point. The main reason could be because this model has been trained on explicit saliency judgments in which observers were asked to click on salient regions. It is not clear whether subjects are able to discover high-level factors that are known to direct gaze (e.g., gaze direction (Borji et al., 2014)). Thus, we believe mining behavioral factors that guide attention and gaze is very valuable in constructing more predictive fixation prediction models.

7. Conclusion

Previous research has shown that humans are capable of automatic and rapid analysis of scene structure when navigating an environment or searching for objects. It has also been shown that several global scene properties such as *coarse spatial layout* (Schyns & Oliva, 1994), *naturalness* (Joubert et al., 2007), *navigability* (Greene & Oliva, 2009), *complexity or clutter* (Sanocki & Sulman, 2009; Rosenholtz et al., 2007), *distance and depth* (Sanocki, 2003), and *openness* (Torralba et al., 2006) can be perceived in a short presentation of a scene. Inspired by these findings, we showed that a particular type of scene structure related to the scene layout, known as the vanishing point, strongly influences eye movements in free viewing of natural scenes as well as in visual search. Our results align with the findings that structural scene information influence gaze guidance during visual search (e.g., Henderson et al. (2009)) and free-viewing (e.g., Le Meur (2011)) and generalize the previous finding that gaze is guided to the road tangent point during driving (Land & Lee, 1994; Land & Tatler, 2001).

In the first experiment, we showed that the density of fixations around the vanishing point is significantly higher than the density of fixations around random locations. This indicates that observers are more likely to look at objects near the vanishing point. We also proposed a combined model made of bottom-up saliency and vanishing point and showed that it outperforms original models. This supports that vanishing point offers significant additional value than what bottom-up saliency already offers. Further, we showed that VP performs significantly above chance and can not be explained by center bias. Since vanishing point commonly occurs in natural vision, we believe that adding this channel to saliency models can boost their prediction power in general scenarios.

In the second experiment, we showed that vanishing point guides attention during visual search and complements other factors involved in target search including spatial context and local object information. Subjects were faster and more accurate when the target character happened near the vanishing point compared to other locations in the image. Results of our two experiments, together support the hypothesis that vanishing point, similar to face and text (Cerf et al., 2009) and gaze direction (Borji et al., 2014; Parks et al., 2015) attracts eye movements and attention in free-viewing and visual search tasks and should be considered in constructing more predictive saliency models.

One interesting future research direction is studying neurophysiological underpinnings of vanishing point detection and guidance in the brain using cell recording and fMRI techniques. It would be also rewarding to find out which cues human observers prioritize, to pay attention to, among several cues such as face, text, gaze direction, vanishing point, etc.

Commercial relationships: None
Corresponding author: Ali Borji
Email: aborji@crcv.ucf.edu
Address: Center for Research in Computer Vision, Department of Computer Science, University of Central Florida, Orlando, USA

References

Ballard, D. H., Hayhoe, M. M., & Pelz, J. B. (1995). Memory representations in natural tasks. *Cognitive Neuroscience, Journal of*, *7*, 66–80.

Bichot, N. P., Rossi, A. F., & Desimone, R. (2005). Parallel and serial neural mechanisms for visual search in macaque area v4. *Science*, *308*, 529–534.

Blaser, E., Sperling, G., & Lu, Z.-L. (1999). Measuring the amplification of attention. *Proceedings of the National Academy of Sciences*, *96*, 11681–11686.

Borji, A., Frintrop, S., Sihite, D. N., & Itti, L. (2012). Adaptive object tracking by learning background context. In *Computer Vision and Pattern Recognition Workshops (CVPRW), 2012 IEEE Computer Society Conference on* (pp. 23–30). IEEE.

Borji, A., & Itti, L. (2012). Exploiting local and global patch rarities for saliency detection. In *Computer Vision and Pattern Recognition (CVPR), 2012 IEEE Conference on* (pp. 478–485). IEEE.

Borji, A., & Itti, L. (2013). State-of-the-art in visual attention modeling. *Pattern Analysis and Machine Intelligence, IEEE Transactions on*, *35*, 185–207.

Borji, A., & Itti, L. (2014a). Defending yarbus: Eye movements reveal observers' task. *Journal of vision*, *14*, 29–29.

Borji, A., & Itti, L. (2014b). Optimal attentional modulation of a neural population. *Frontiers in computational neuroscience*, *8*.

Borji, A., Parks, D., & Itti, L. (2014). Complementary effects of gaze direction and early saliency in guiding fixations during free viewing. *Journal of vision*, *14*, 3–3.

Borji, A., Sihite, D. N., & Itti, L. (2013a). Objects do not predict fixations better than early saliency: A re-analysis of einhäuser et al.'s data. *Journal of vision*, *13*, 18–18.

Borji, A., Sihite, D. N., & Itti, L. (2013b). Quantitative analysis of human-model agreement in visual saliency modeling: a comparative study. *Image Processing, IEEE Transactions on*, *22*, 55–69.

Borji, A., & Tanner, J. (2015). Reconciling saliency and object center-bias hypotheses in explaining free-viewing fixations, .

Bruce, N., & Tsotsos, J. (2005). Saliency based on information maximization. In *Advances in neural information processing systems* (pp. 155–162).

Bylinskii, Z., Isola, P., Bainbridge, C., Torralba, A., & Oliva, A. (2015). Intrinsic and extrinsic effects on image memorability. *Vision research*, *116*, 165–178.

Bylinskii, Z., Judd, T., Durand, F., Oliva, A., & Torralba, A. (2014). Mit saliency benchmark.

Castelhano, M. S., Wieth, M., & Henderson, J. M. (2007). I see what you see: Eye movements in real-world scenes are affected by perceived direction of gaze. In *Attention in cognitive systems. Theories and systems from an interdisciplinary viewpoint* (pp. 251–262). Springer.

Cerf, M., Frady, E. P., & Koch, C. (2009). Faces and text attract gaze independent of the task: Experimental data and computer model. *Journal of vision*, *9*, 10–10.

Chattington, M., Wilson, M., Ashford, D., & Marple-Horvat, D. (2007). Eye–steering coordination in natural driving. *Experimental brain research*, *180*, 1–14.

Chen, X., & Zelinsky, G. J. (2006). Real-world visual search is dominated by top-down guidance. *Vision research*, *46*, 4118–4133.

Chua, H. F., Boland, J. E., & Nisbett, R. E. (2005). Cultural variation in eye movements during scene perception. *Proceedings of the National Academy of Sciences of the United States of America*, *102*, 12629–12633.

Cortes, C., & Vapnik, V. (1995). Support-vector networks. *Machine learning*, *20*, 273–297.

Coughlan, J. M., & Yuille, A. L. (2003). Manhattan world: Orientation and outlier detection by bayesian inference. *Neural Computation*, *15*, 1063–1088.

Ehinger, K. A., Hidalgo-Sotelo, B., Torralba, A., & Oliva, A. (2009). Modelling search for people in 900 scenes: A combined source model of eye guidance. *Visual cognition*, *17*, 945–978.

Friedman, A. (1979). Framing pictures: the role of knowledge in automatized encoding and memory for gist. *Journal of experimental psychology: General*, *108*, 316.

Greene, M. R., & Oliva, A. (2009). The briefest of glances the time course of natural scene understanding. *Psychological Science*, *20*, 464–472.

Hayhoe, M., & Ballard, D. (2005). Eye movements in natural behavior. *Trends in cognitive sciences*, *9*, 188–194.

Henderson, J. M., Chanceaux, M., & Smith, T. J. (2009). The influence of clutter on real-world scene search: Evidence from search efficiency and eye movements. *Journal of Vision*, *9*, 32–32.

Hoiem, D., Efros, A. A., & Hebert, M. (2005). Geometric context from a single image. In *Computer Vision, 2005. ICCV 2005. Tenth IEEE International Conference on* (pp. 654–661). IEEE volume 1.

Hwang, A. D., Wang, H.-C., & Pomplun, M. (2011). Semantic guidance of eye movements in real-world scenes. *Vision research*, *51*, 1192–1205.

Itti, L., Koch, C., & Niebur, E. (1998). A model of saliency-based visual attention for rapid scene analysis. *IEEE Transactions on Pattern Analysis & Machine Intelligence*, (pp. 1254–1259).

Jiang, M., Huang, S., Duan, J., & Zhao, Q. (2015). Salicon: Saliency in context. In *Computer Vision and Pattern Recognition (CVPR), 2015 IEEE Conference on* (pp. 1072–1080). IEEE.

Joubert, O. R., Rousselet, G. A., Fize, D., & Fabre-Thorpe, M. (2007). Processing scene context: Fast categorization and object interference. *Vision research*, *47*, 3286–3297.

Judd, T., Durand, F., & Torralba, A. (2012). A benchmark of computational models of saliency to predict human fixations, .

Kenner, N., & Wolfe, J. M. (2003). An exact picture of your target guides visual search better than any other representation. *Journal of Vision*, *3*, 230–230.

Koch, C., & Ullman, S. (1987). Shifts in selective visual attention: towards the underlying neural circuitry. In *Matters of intelligence* (pp. 115–141). Springer.

Land, M. F., & Lee, D. N. (1994). Where do we look when we steer. *Nature*, .

Land, M. F., & Tatler, B. W. (2001). Steering with the head: The visual strategy of a racing driver. *Current Biology*, *11*, 1215–1220.

Le Meur, O. (2011). Predicting saliency using two contextual priors: the dominant depth and the horizon line. In *Multimedia and Expo (ICME), 2011 IEEE International Conference on* (pp. 1–6). IEEE.

Martinez-Trujillo, J. C., & Treue, S. (2004). Feature-based attention increases the selectivity of population responses in primate visual cortex. *Current Biology*, *14*, 744–751.

Maxfield, J. T., Stalder, W. D., & Zelinsky, G. J. (2014). Effects of target typicality on categorical search. *Journal of vision*, *14*, 1–1.

McCarthy, G., Puce, A., Gore, J. C., & Allison, T. (1997). Face-specific processing in the human fusiform gyrus. *Journal of cognitive neuroscience*, *9*, 605–610.

Navalpakkam, V., & Itti, L. (2005). Modeling the influence of task on attention. *Vision research*, *45*, 205–231.

Navalpakkam, V., & Itti, L. (2006). An integrated model of top-down and bottom-up attention for optimizing detection speed. In *Computer Vision and Pattern Recognition, 2006 IEEE Computer Society Conference on* (pp. 2049–2056). IEEE volume 2.

Navalpakkam, V., & Itti, L. (2007). Search goal tunes visual features optimally. *Neuron*, *53*, 605–617.

Nuthmann, A., & Henderson, J. M. (2010). Object-based attentional selection in scene viewing. *Journal of vision*, *10*, 20–20.

Oliva, A., & Torralba, A. (2001). Modeling the shape of the scene: A holistic representation of the spatial envelope. *International journal of computer vision*, *42*, 145–175.

Ouerhani, N., & Hügli, H. (2000). Computing visual attention from scene depth. In *Pattern Recognition, 2000. Proceedings. 15th International Conference on* (pp. 375–378). IEEE volume 1.

Parkhurst, D., Law, K., & Niebur, E. (2002). Modeling the role of salience in the allocation of overt visual attention. *Vision research*, *42*, 107–123.

Parks, D., Borji, A., & Itti, L. (2015). Augmented saliency model using automatic 3d head pose detection and learned gaze following in natural scenes. *Vision research*, *116*, 113–126.

Peters, R. J., Iyer, A., Itti, L., & Koch, C. (2005). Components of bottom-up gaze allocation in natural images. *Vision research*, *45*, 2397–2416.

Potter, M. C. (1976). Short-term conceptual memory for pictures. *Journal of experimental psychology: human learning and memory*, *2*, 509.

Rayner, K., Castelhano, M. S., & Yang, J. (2009). Eye movements when looking at unusual/weird scenes: Are there cultural differences? *Journal of Experimental Psychology: Learning, Memory, and Cognition*, *35*, 254.

Rensink, R. A. (2000). The dynamic representation of scenes. *Visual cognition*, *7*, 17–42.

Rosenholtz, R., Li, Y., & Nakano, L. (2007). Measuring visual clutter. *Journal of vision*, *7*, 17–17.

Ross, M. G., & Oliva, A. (2009). Estimating perception of scene layout properties from global image features. *Journal of vision*, *10*, 2–2.

Saenz, M., Buracas, G. T., & Boynton, G. M. (2002). Global effects of feature-based attention in human visual cortex. *Nature neuroscience*, *5*, 631–632.

Sanocki, T. (2003). Representation and perception of scenic layout. *Cognitive Psychology*, *47*, 43–86.

Sanocki, T., & Sulman, N. (2009). Priming of simple and complex scene layout: Rapid function from the intermediate level. *Journal of Experimental Psychology: Human Perception and Performance*, *35*, 735.

Schyns, P. G., & Oliva, A. (1994). From blobs to boundary edges: Evidence for time-and spatial-scale-dependent scene recognition. *Psychological science*, *5*, 195–200.

Tanenhaus, M. K., Spivey-Knowlton, M. J., Eberhard, K. M., & Sedivy, J. C. (1995). Integration of visual and linguistic information in spoken language comprehension. *Science*, *268*, 1632–1634.

Tatler, B. W., Baddeley, R. J., & Gilchrist, I. D. (2005). Visual correlates of fixation selection: effects of scale and time. *Vision research*, *45*, 643–659.

Torralba, A., Oliva, A., Castelhano, M. S., & Henderson, J. M. (2006). Contextual guidance of eye movements and attention in real-world scenes: the role of global features in object search. *Psychological review*, *113*, 766.

Treisman, A. M., & Gelade, G. (1980). A feature-integration theory of attention. *Cognitive psychology*, *12*, 97–136.

Treue, S., & Trujillo, J. C. M. (1999). Feature-based attention influences motion processing gain in macaque visual cortex. *Nature*, *399*, 575–579.

Triesch, J., Ballard, D. H., Hayhoe, M. M., & Sullivan, B. T. (2003). What you see is what you need. *Journal of vision*, *3*, 9–9.

Tseng, P.-H., Carmi, R., Cameron, I. G., Munoz, D. P., & Itti, L. (2009). Quantifying center bias of observers in free viewing of dynamic natural scenes. *Journal of vision*, *9*, 4–4.

Wilson, M., Chattington, M., & Marple-Horvat, D. E. (2008). Eye movements drive steering: Reduced eye movement distribution impairs steering and driving performance. *Journal of motor behavior*, *40*, 190–202.

Wolfe, J. M. (2007). Guided search 4.0. *Integrated models of cognitive systems*, (pp. 99–119).

Yang, C., Zhang, L., Lu, H., Ruan, X., & Yang, M.-H. (2013). Saliency detection via graph-based manifold ranking. In *Proceedings of the IEEE Conference on Computer Vision and Pattern Recognition* (pp. 3166–3173).

Yarbus, A. L., Haigh, B., & Rigss, L. A. (1967). Eye movements and vision (vol. 2). *Plenum press New York*, *2*, 7.

Zelinsky, G. J. (2008). A theory of eye movements during target acquisition. *Psychological review*, *115*, 787.

Zhang, J., & Sclaroff, S. (2013). Saliency detection: A boolean map approach. In *Proceedings of the IEEE International Conference on Computer Vision* (pp. 153–160).

8. Appendix A

Figure 9 shows the consistency results of our two annotators in marking the vanishing point location. Each point is the location of an annotated VP in the image. R^2 is correlation coefficient of the 2D vectors. The bar chart shows the distribution of annotation differences between the two subjects. For about 280 of the images (out of 319), the difference is smaller than or equal to 5 pixels on a 640×480 pixel image. Since annotators were very consistent, we used annotations of only one of them in our analyses.

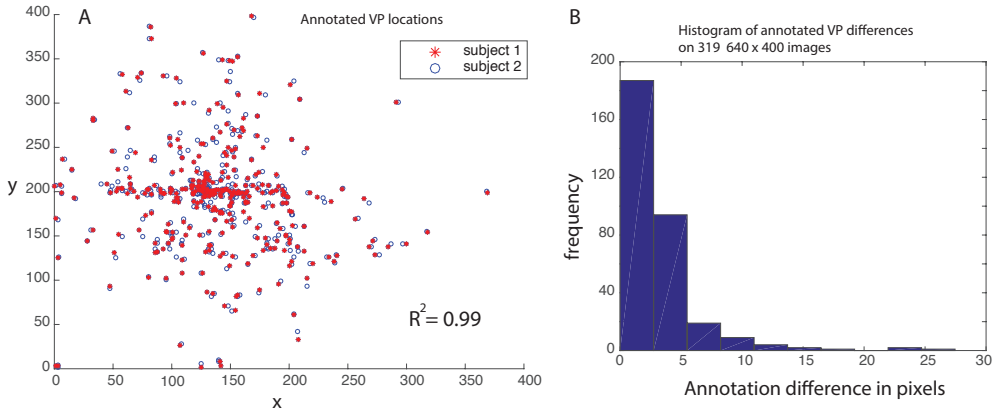

Figure 9: A) Annotated VP locations by two annotator, B) Histogram of vanishing point differences.

9. Appendix B

Figure 10 shows the response time and accuracy of subjects in the visual search experiment.

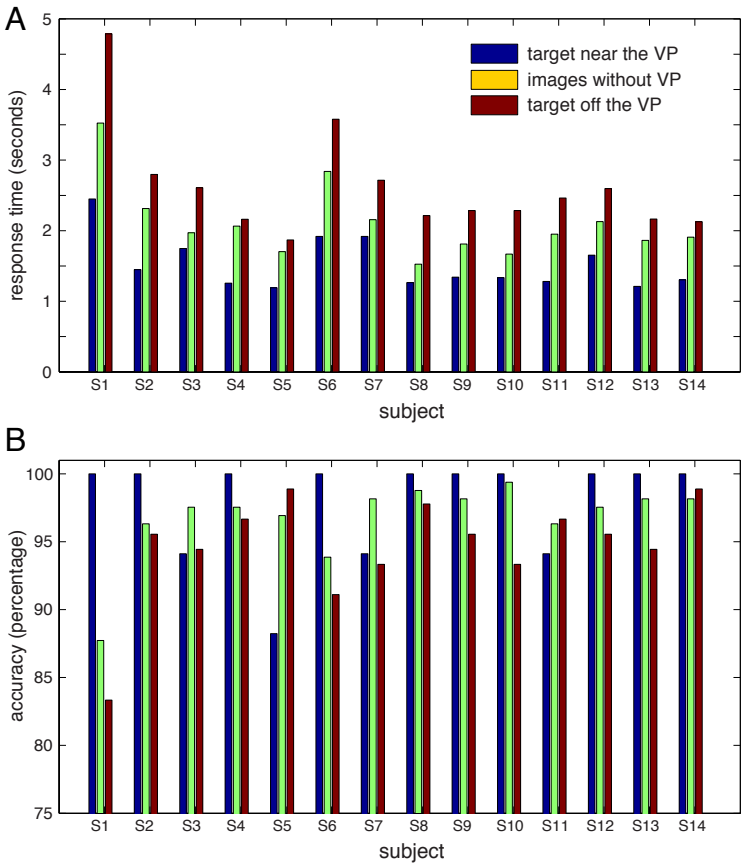

Figure 10: Response time (A) and accuracy (B) of subjects in the visual search experiment.